Natural convection and surface thermal radiation in a tilted open shallow cavity

J.F. Hinojosa Palafox
University of Sonora, Hermosillo, Sonora, México,
Blvd. Rosales y Luis Encinas s/n, 83000,
e-mail: fhinojosa@iq.uson.mx

Recibido el 19 de septiembre de 2011; aceptado el 2 de diciembre de 2011

In this paper the numerical calculations of heat transfer by natural convection and surface radiation in a tilted open shallow cavity are presented. The cavity maintains the opposite wall to the aperture at a constant temperature while the remaining walls are adiabatic. The results in the steady state are obtained for a Rayleigh number range from 10^5 to 10^7, inclination angles from 45° to 135° and aspect ratios equal to 2 and 4. It was found that the exchange of thermal radiation between walls is considerably more relevant that the convective phenomenon for an inclination angle of 135°. Oscillations in the convective Nusselt number were observed for inclination angles of 45° (AR=4) and 90° (AR of 2 and 4) caused by the formation of thermal plumes in the bottom adiabatic wall that travel and mix with the thermal layer of the hot wall.

Keywords: Shallow open cavity; natural convection; thermal radiation.

PACS: 44.25.+f; 44.40.+a

1. Introduction

The heat transfer in open cavities is relevant in several thermal engineering applications, for example in the cooling of electronic devices and the design of solar concentrators receivers, among others. In the thermosolar system of parabolic dish with a Stirling thermal engine used to produce electricity, the solar concentrator has a tracking system to maintain its optical axis pointing directly towards the sun. During the tracking, the receiver (open cavity) located at the focal point of the concentrator operates with different inclination angles. The rotation modifies the air motion pattern and the thermal field in the open cavity. However the heat losses in the open cavity receiver are mainly by the heat transfer mechanisms of convection and thermal radiation, therefore it is important to fully understand the basic behavior of these heat transfer mechanisms.

In the literature a large number of numerical studies have been reported to describe the heat transfer in open cavities [1-35]. These studies can be categorized as: (a) natural convection in an open cavity with isothermal walls, (b) natural convection in an open cavities with adiabatic walls and isothermal at the wall facing the aperture, (c) combined natural convection with conduction or surface thermal radiation in two-dimensional open cavities [9,11-12,21-22,24-26], (d) natural convection in partially open cavities [6,15,23,27] and (e) natural convection in a cavity with two open sides (using a symmetry plane) [7-8,17-19,31,33]. The investigations of the heat transfer by combined natural convection and surface thermal radiation are briefly presented next.

Lage *et al.*, [9] studied numerically the heat transfer by natural convection and surface thermal radiation in a two-dimensional open top cavity; the numerical approach used by the authors consisted of solving separately the steady state equations of natural convection and thermal radiation, assuming a temperature distribution on the vertical adiabatic wall. Balaji and Venkateshan [11] obtained steady state numerical results for the interaction of surface thermal radiation with free convection in an open top cavity, whose left wall was considered isothermal, and the right and bottom walls were adiabatic and their temperature distributions were determined by an energy balance between convection and radiation in each surface element of the walls. Surface radiation was found to alter the basic flow pattern as well as the overall thermal performance substantially. Balaji and Venkateshan [12] made a numerical study of combined conduction, natural convection and surface thermal radiation in an open top cavity. The authors reports a numerical correlation based on the numerical results. Radiation was found to enhance overall heat transfer substantially (50–80%) depending on the radiative parameters

Singh and Venkateshan [22] presented a numerical study of steady combined laminar natural convection and surface radiation in a two-dimensional side-vented open cavity. Surface radiation is found to alter the basic flow pattern as well as the thermal performance substantially. The numerical investigation provides evidence of the existence of thermal boundary layers along adiabatic walls of the cavity as a consequence of the interaction of natural convection and surface radiation. Hinojosa *et al.*, [24] reported numeric results of Nusselt numbers for a tilted open square cavity, considering natural convection and surface thermal radiation. The results were obtained for a Rayleigh range from 10^4 to 10^7 and for an inclination angles range of the cavity from 0° to 180°. The results show that convective Nusselt number changes substantially with the inclination angle of the cavity, while the radiative Nusselt number is insensitive to the orientation change of the cavity. Hinojosa *et al.* [26] presented numerical results for transient and steady-state natural convection and surface thermal radiation in a horizontal open square cavity. The results show that the radiative exchange between the walls and the aperture increases considerably the total average Nusselt

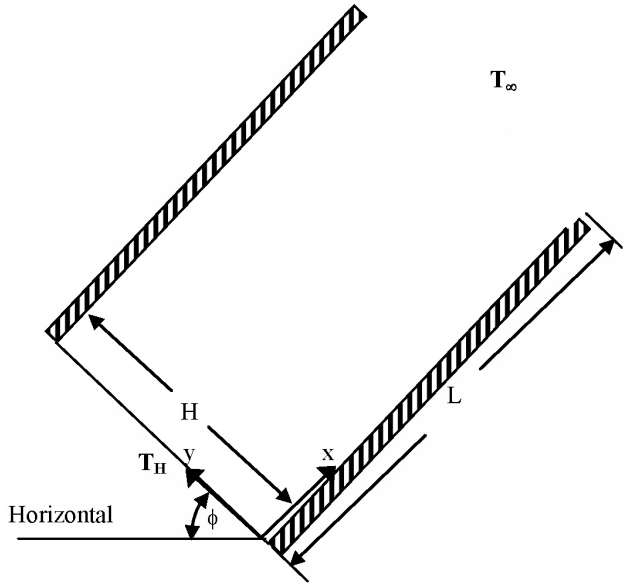

FIGURE 1. Scheme of the tilted open shallow cavity.

number, from around 94% to 125%. Nouanegue *et al.* [27] investigated conjugate heat transfer by natural convection, conduction and radiation in open cavities in which a uniform heat flux is applied to the inside surface of the solid wall facing the opening. The influence of the surface radiation is to decrease the heat fluxes by natural convection and conduction while the heat flux by radiation increases with increasing surface emissivity.

However the previous works has not studied the effect of the inclination angle of the heat transfer by natural convection and surface thermal radiation in shallow open cavities. Considering above this work focuses in the numerical analysis of the fluid motion pattern, the temperature field and heat transfer in a tilted open shallow cavity for a Rayleigh range from 10^5 to 10^7, an inclination angle range from 45° to 135° and aspect ratios equal to 2 and 4, solving simultaneously the natural convection and the surface thermal radiation.

2. Physical problem and mathematical model

The heat transfer in a two dimensional tilted open shallow cavity is considered in this paper as shown in Fig. 1. The opposite wall to the aperture was kept at a constant temperature T_H, while the surrounding fluid interacting with the aperture was fixed to an ambient temperature T_∞. The two remaining walls were insulated. The fluid was air and the fluid flow was laminar. The fluid was radiatively non-participating and the walls of the cavity were considered as black bodies. The properties of the fluid were considered constant except for the density in the buoyant force term in the momentum equations, according to the Boussinesq approximation. Because radiative calculations are carried out the temperatures of isothermal wall and ambient were fixed to 310 K and 300 K, respectively, guaranteeing Boussinesq approximation.

From the above considerations, the transient state dimensionless conservation equations governing the transport of mass, momentum, and energy in primitive variables are expressed as:

$$\frac{\partial U}{\partial X}+\frac{\partial V}{\partial Y}=0 \tag{1}$$

$$\frac{\partial U}{\partial \tau}+\frac{\partial\left(U^2\right)}{\partial X}+\frac{\partial\left(UV\right)}{\partial Y}=-\frac{\partial P}{\partial X}+\left(\frac{\Pr}{Ra}\right)^{1/2}\left(\frac{\partial^2 U}{\partial X^2}+\frac{\partial^2 U}{\partial Y^2}\right)+\theta\,\cos\phi \tag{2}$$

$$\frac{\partial V}{\partial \tau}+\frac{\partial\left(UV\right)}{\partial X}+\frac{\partial\left(V^2\right)}{\partial Y}=-\frac{\partial P}{\partial Y}+\left(\frac{\Pr}{Ra}\right)^{1/2}\left(\frac{\partial^2 V}{\partial X^2}+\frac{\partial^2 V}{\partial Y^2}\right)+\theta\,\sin\phi \tag{3}$$

$$\frac{\partial \theta}{\partial \tau}+\frac{\partial\left(U\theta\right)}{\partial X}+\frac{\partial\left(V\theta\right)}{\partial Y}=\frac{1}{\left(\Pr\, Ra\right)^{1/2}}\left(\frac{\partial^2 \theta}{\partial X^2}+\frac{\partial^2 \theta}{\partial Y^2}\right) \tag{4}$$

where Ra=[gβ(T_H-T_∞)L^3]/$\alpha\nu$ is the Rayleigh number, and Pr=ν/α is the Prandtl number. The dimensionless variables were defined as:

$$\begin{aligned} &X=x/L,\quad Y=y/H,\quad \tau=U_o t/L,\\ &P=(p-p_\infty)/\rho U_o^2,\\ &U=u/U_o,\quad V=v/U_o,\quad \theta=(T-T_\infty)/(T_H-T_\infty)\end{aligned} \tag{5}$$

the reference velocity U_o is related to the buoyancy force term and was defined as $U_o=\left(g\beta L(T_H-T_\infty)\right)^{1/2}$ [6].

The initial and boundary conditions were taken as follow:

$$P(X,Y,0)=U(X,Y,0)=V(X,Y,0)=\theta(X,Y,0)=0 \tag{6}$$

$$U(0,Y,\tau)=V(0,Y,\tau)=U(X,0,\tau)=V(X,0,\tau)=U(X,1,\tau)=V(X,1,\tau)=0 \tag{7}$$

$$\left(\frac{\partial U}{\partial X}\right)_{X=AR}=\left(\frac{\partial V}{\partial X}\right)_{X=AR}=0 \tag{8}$$

$$\theta(0,Y,\tau)=1 \tag{9}$$

$$\theta(AR,Y,\tau)=0 \quad \text{if} \quad U<0$$

$$\text{or} \quad \left(\frac{\partial \theta}{\partial X}\right)_{X=AR}=0 \quad \text{if} \quad U>0 \tag{10}$$

$$\left(\frac{\partial \theta}{\partial Y}\right)_{Y=0,1}=N_r Q_r \tag{11}$$

where $N_r=\sigma T_H^4 L/k\,(T_H-T_\infty)$, is the dimensionless parameter of conduction-radiation, $Q_r=q_r/\sigma T_H^4$ is the dimensionless net radiative heat flux on the corresponding insulated wall and AR=L/H is the aspect ratio of the cavity. The initial condition given by Eq. (6), considers a stagnated fluid at am-

TABLE I. Comparison of the heat transfer results for the natural convection in a tilted square shallow cavity with AR=2.

Mohamad [13]				
ϕ	**Ra**			
	$\mathbf{10^4}$	$\mathbf{10^5}$	$\mathbf{10^6}$	$\mathbf{10^7}$
10°	2.21±0.2	3.10±0.24	11.38±2.6	—
30°	3.07	6.38	10.6±3.0	—
60°	3.43	7.35	14.04	—
90°	2.62	7	14.21	26.82
This work				
ϕ	**Ra**			
	$\mathbf{10^4}$	$\mathbf{10^5}$	$\mathbf{10^6}$	$\mathbf{10^7}$
10°	2.47	4.2±0.23	11.39±1.60	23.28±2.15
30°	3.21	6.42	12.18±1.23	22.98±0.20
60°	3.41	7.39	14.23	26.79±0.01
90°	2.58	7.07	14.57	27.93

bient pressure and temperature. In the hydrodynamic boundary conditions, Eq. (7) assumes non-slip behavior at the solid walls, whereas Eq. (8) assumes that in the aperture plane no velocity gradients and thus no momentum transfer occurs at this location. In the thermal boundary conditions, Eq. (9) corresponds to the isothermal wall, for the aperture plane the Eq. (10) considered that the incoming fluid enters to the cavity at ambient temperature, while for the fluid leaving the cavity the thermal conduction is despicable; finally Eq. (11) was obtained applying an energy balance on the adiabatic surfaces by considering the transmission of heat by radiation and convection.

To obtain the net radiative heat fluxes over the walls, the walls were divided in elements according to the mesh used to solve Eqs. (1)-(4) and the radiosity-irradiance formulation was applied. The general radiosity equation for the ith element of the cavity may be written as:

$$J_i = \varepsilon_i \sigma T_i^4 + (1-\varepsilon_i)\sum_{j=1}^{N} F_{ij} J_j \tag{12}$$

where, ε_i is the emissivity of the surface element; F_{ij} is the view factor from the ith element to the jth element of the cavity, while N is the total number of elements along the cavity. View factors were evaluated using Hottel's crossed string method [13]. The net radiative flux (q_r) for the ith element of any of the walls of the cavity was calculated by:

$$\mathrm{q}_{ri} = \mathrm{J}_i - \mathrm{q}_{Ii} \tag{13}$$

where q_{ri} is the net radiative heat flux, J_i is the radiosity of the corresponding element and q_{Ii} is the irradiance energy that arrives to the ith element coming from the rest of the elements of the cavity.

The average convective Nusselt number was calculated integrating the temperature gradient over the isothermal wall as:

$$\overline{Nu}_c = \int_0^1 -\frac{\partial\theta}{\partial X} dY \tag{14}$$

The average radiative Nusselt number was obtained integrating the dimensionless net radiative fluxes over the isothermal wall, by the following mathematical relationship:

$$\overline{Nu}_r = N_r \int_0^1 Q_r dY \tag{15}$$

The total average Nusselt number was calculated by summing the average convective Nusselt number and the average radiative Nusselt number:

$$\overline{Nu}_t = \overline{Nu}_c + \overline{Nu}_r = \int_0^1 -\frac{\partial\theta}{\partial X} dY + N_r \int_0^1 Q_r dY \tag{16}$$

3. Numerical method of solution

The Eqs. (1)-(4) were discretized using staggered and uniform control volumes. For the discretization of the convective terms was used the SMART scheme [29] and for the diffusive terms the central differencing scheme. The fully implicit scheme was used for the time discretization. The SIMPLEC algorithm [30] was applied to couple continuity and momentum equations. The resulting system of linear algebraic equations was solved iteratively by the SIP method [31]. Due to the coupling between the natural convection and the surface thermal radiation, the radiative exchange between walls was solved in every time step using an iterative method of subsequent approaches. After an independence mesh study, the results were obtained with the following grid meshes: 200×100 (AR=2) and 400×100 (AR=4). The dimensionless time step used for the calculations was 1×10^{-3}.

4. Results

In order to verify the numerical code, the pure natural convection in a tilted open shallow cavity was solved and the results were compared with the ones reported by Mohamad [13]. In Table I the comparison between the average Nusselt numbers is presented for AR=2, it shows that the highest percentage

TABLE II. Verification results of the surface thermal radiative model.

Wall	This Work [W m^{-2}]	Sanchez and Smith [18] [W m^{-2}]	Difference (%)
Vertical	64.365	—-	
Top horizontal	-18.853	-18.849	0.02
Aperture	-26.661	-26.657	0.01
Bottom horizontal	-18.853	-18.849	0.02

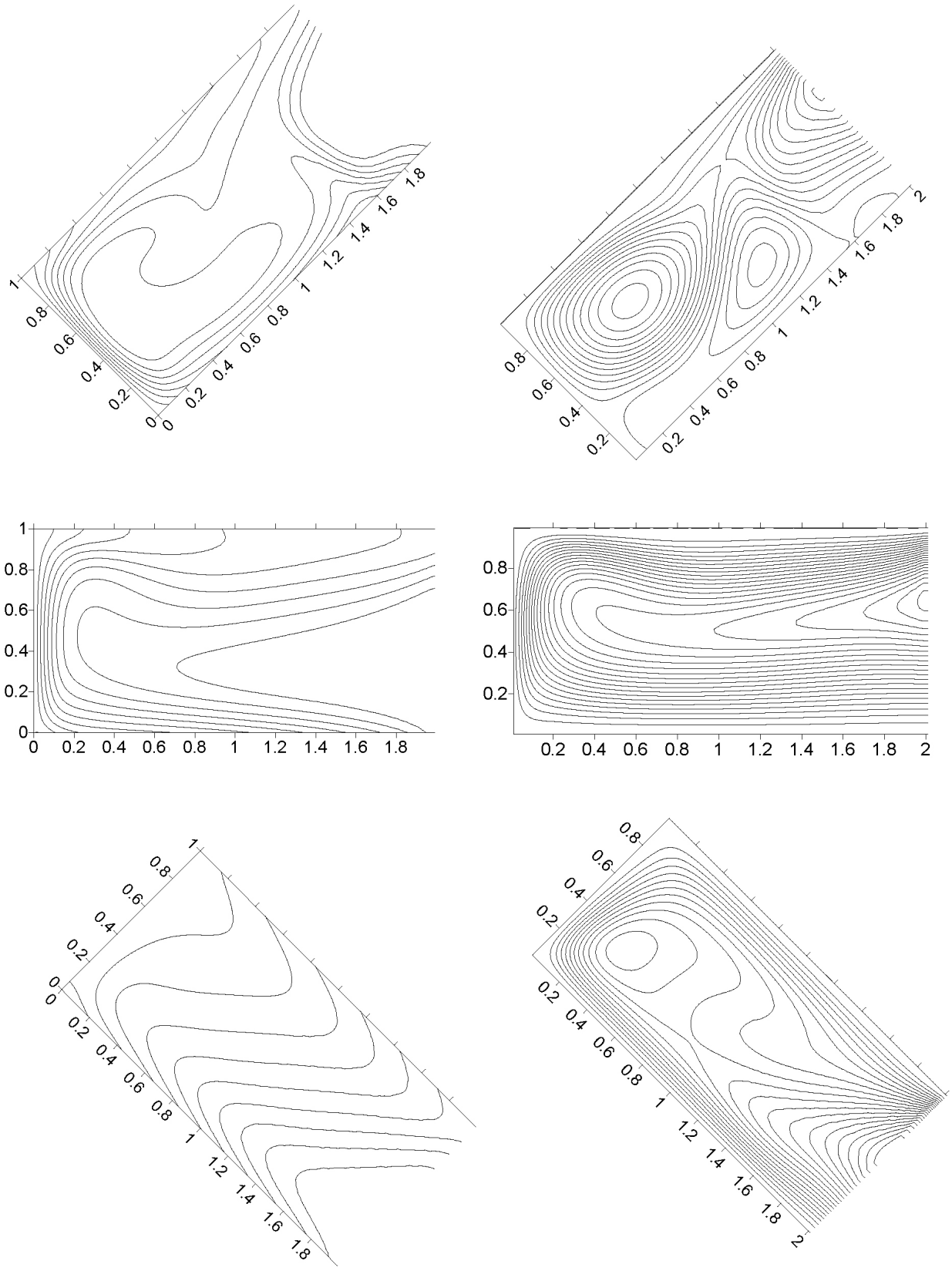

FIGURE 2. Isotherms (left) and streamlines (right) for AR=2, Ra=10^5 and three inclination angles of the open cavity (45°, 90° and 135°).

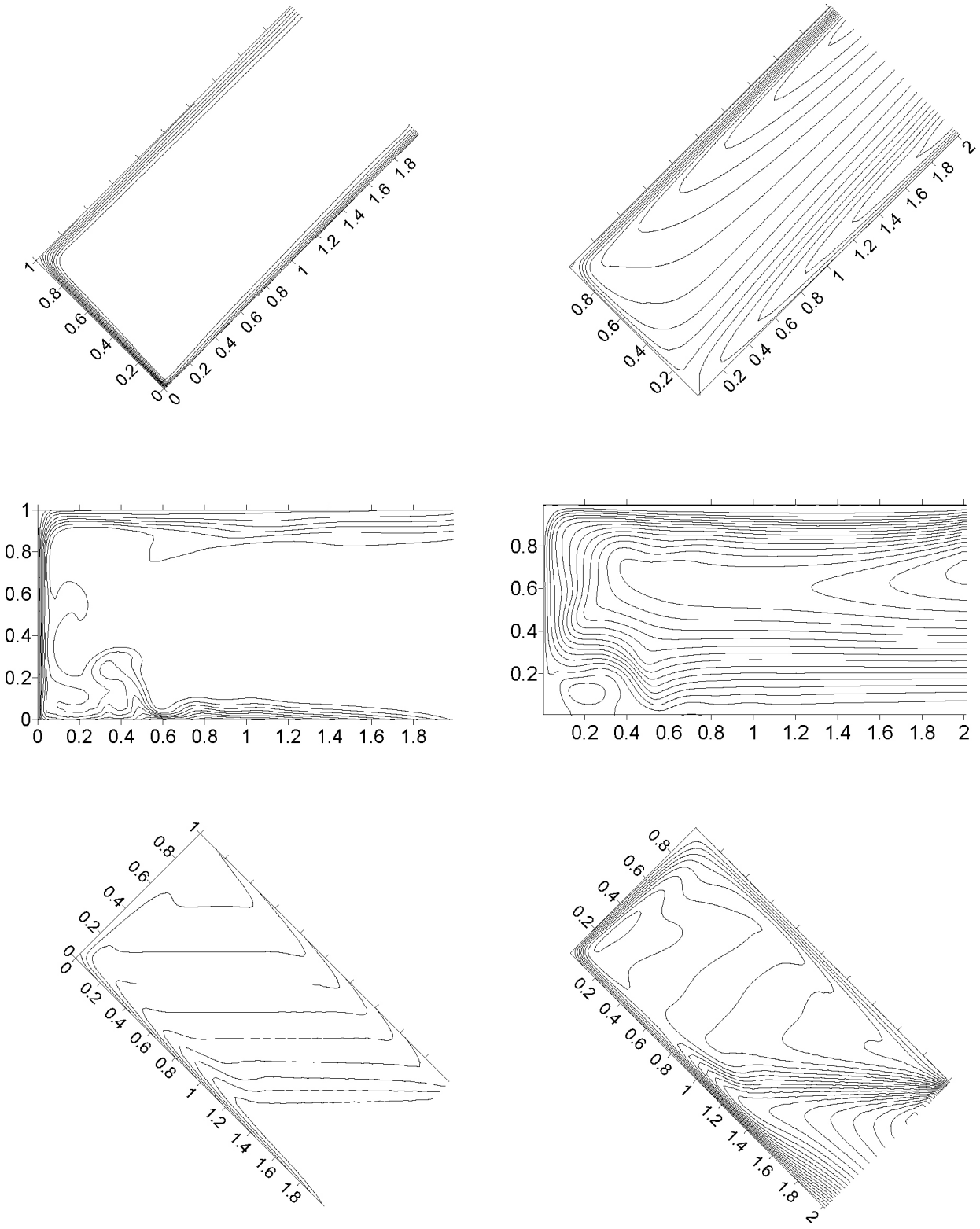

FIGURE 3. Isotherms (left) and streamlines (right) for AR=2, Ra=10^7 and three inclination angles of the open cavity (45°, 90° and 135°).

difference was 4.56% for Ra =10^4 and ϕ=30°; whereas the lowest was 0.54% for Ra =10^5 and ϕ=60°, with an average percentage difference of 1.87%. The surface thermal radiative model was validated by comparing the results with the ones of Sanchez and Smith [32], to do so, the natural convection was suppressed and the temperature of the vertical wall of the cavity was fixed at 310 K, while the two horizontal walls and the aperture were maintained to a constant temper-

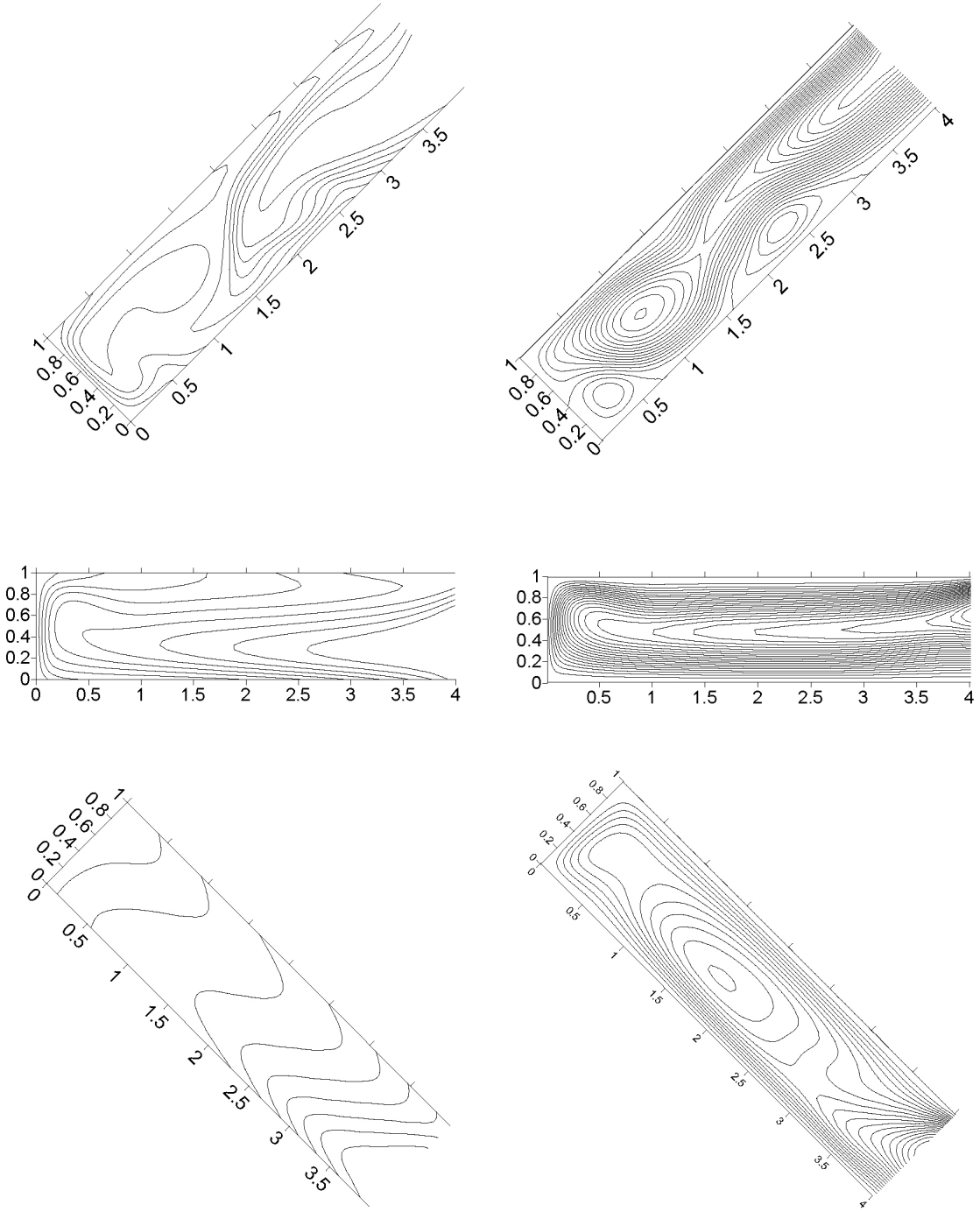

FIGURE 4. Isotherms (left) and streamlines (right) for AR=4, Ra=10^5 and three inclination angles of the open cavity (45°, 90° and 135°).

ature of 300 K. The three isothermal walls were considered as gray bodies (with ε=1). The comparison between the dimensional surface radiative fluxes of this work and the ones of Sanchez and Smith is presented in Table II. The maximum percentage difference was 0.02%. The good agreement between the predictions of the present code and those reported in the literature verifies the validity of the computational code.

The numerical results of the combined natural convection and surface thermal radiation, for Rayleigh numbers of Ra=$10^5$and Ra=10^7, aspect ratios of 2 and 4 and three inclination angles (45°, 90° and 135°) are shown and discussed next. The fluid flow patterns are reported using streamlines graphs, whereas the temperature fields are shown using isotherms graphs.

The corresponding results for an aspect ratio of 2 and Rayleigh number of 10^5 are presented in Fig. 2. It is appreciated from graphs that the temperature field and the flow pattern are very sensitive to the orientation of the cavity. For an inclination angle of 45°, in the graph of streamline two vor-

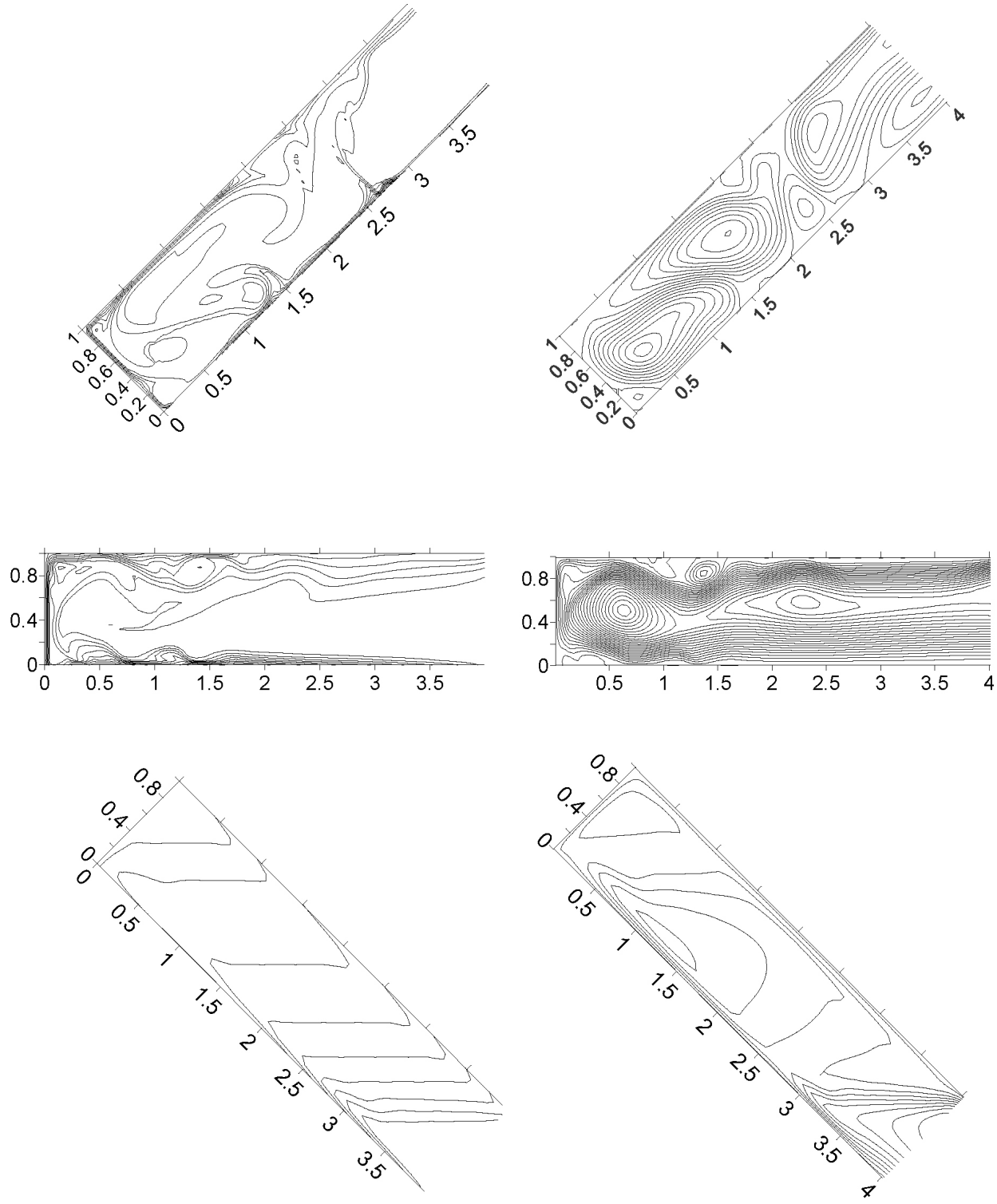

FIGURE 5. Isotherms (left) and streamlines (right) for AR=4, Ra=10^7 and three inclination angles of the open cavity (45°, 90° and 135°).

texes are observed, the smaller one coincides with the thermal plume arising from the bottom adiabatic wall observed in the graph of isotherms, this thermal plume is formed because the entering air is heated from below by the bottom adiabatic wall; the second vortex is moving up impelled by the buoyancy force. When the cavity has an inclination angle of 90°, the graph of streamlines indicates that the fluid moves around the cavity, entering by the low section of the aperture and leaving by the top section, in the graph of isotherms can be seen that the bottom adiabatic wall is heated by the radiative exchange. However for an inclination angle of 135°, the graph of isotherms shows that the thermal boundary layer ad-

TABLE III. Average values of convective Nusselt (Nu_C), radiative Nusselt (Nu_R) and total Nusselt (Nu_T).

Ra=10^5						
ϕ	AR=2			AR=4		
	$\overline{Nu}_c$	$\overline{Nu}_r$	$\overline{Nu}_t$	$\overline{Nu}_c$	$\overline{Nu}_r$	$\overline{Nu}_t$
45°	5.30	5.63	10.93	2.76	4.14	6.91
90°	4.27	5.63	9.90	2.65	4.17	6.81
135°	0.57	5.62	6.18	0.54	4.13	4.67
Ra=10^6						
ϕ	AR=2			AR=4		
	$\overline{Nu}_c$	$\overline{Nu}_r$	$\overline{Nu}_t$	$\overline{Nu}_c$	$\overline{Nu}_r$	$\overline{Nu}_t$
45°	12.74	12.15	24.89	5.10	8.96	14.06
90°	10.15	12.13	22.28	7.46	8.98	16.44
135°	0.85	12.10	12.95	0.88	8.90	9.78
Ra=10^7						
ϕ	AR=2			AR=4		
	$\overline{Nu}_c$	$\overline{Nu}_r$	$\overline{Nu}_t$	$\overline{Nu}_c$	$\overline{Nu}_r$	$\overline{Nu}_t$
45°	25.54±0.07	26.16	51.70	19.1±2.4	19.40	38.5±2.4
90°	22.33±1.22	26.11	48.44±1.2	18.71±1.88	19.35	38.06±1.88
135°	1.95	26.08	28.03	1.61	19.19	20.8

jacent to the isothermal wall formed for 45° and 90° is not present and a vortex is observed in the graph of streamlines, it reduces the incoming cold fluid that reaches the isothermal wall.

The Fig. 3 presents the numerical results for an aspect ratio of 2 and Rayleigh number of 10^7. It is noted the strong influence of the inclination angle over the temperature field and fluid flow pattern. When the cavity has an inclination angle of 45° the graph of isotherms shows thin boundary layers on the walls, whereas in the graph of streamlines, two zones of fluid circulation are observed, the first zone is located near the bottom adiabatic wall, in this one the incoming air advances but it turns around toward the aperture before reaching the isothermal wall; the second zone is located over the first one, in this case the entering fluid reaches the isothermal wall, turns up impelled by the buoyancy force and goes out by the top section of the cavity. For an inclination angle of 90°, a thermal plume emerging from the bottom adiabatic wall and travelling adjacent to the isothermal wall is observed in the graph of isotherms; while the graph of streamlines shows a vortex corresponding to the previously described thermal plume. If the cavity has an inclination angle of 135°, the graph of streamlines indicates that only a small part of the incoming air reaches the isothermal wall, most of it turns back to the aperture in oblique way; as a consequence the isotherms almost have an oblique shape.

The results for an aspect ratio of 4 and Rayleigh number of 10^5 are presented in Fig. 4. It is appreciated in the graphs that again the temperature field and the flow pattern are very sensitive to the orientation of the cavity. For 45°, the graph of streamlines shows two different movements of the fluid. In the main one the cold fluid comes in by the low section of the aperture, it reaches the isothermal wall and leaves for the upper section of the opening. In the second movement the cold fluid enters by the center of the aperture, but collides with a vortex and goes out without reaching the isothermal wall. On the other hand, there are two more vortexes, one near the middle of the bottom adiabatic wall and another in the lower corner of the cavity. The temperature field behavior observed in the graph of isotherms follows very close the previously described flow pattern, the first three isotherms near to the aperture correspond to the second movement of the fluid, the remaining isotherms to the first movement of the fluid and the vortexes. When the inclination angle is 90°, the flow pattern shown by the graph of streamlines indicates that the cold fluid enters for the bottom section of the aperture, it reaches the hot wall and it leaves for the top section of the opening, following the shape of the cavity. It is also appreciated in the graph of isotherms the effect of the adiabatic walls, because the radiative exchange the temperature of the bottom adiabatic wall is major than that of the incoming fluid, whereas the temperature of the top adiabatic wall is minor than the outgoing air. For an orientation of the cavity of 135°, the fluid flow pattern presented in the graph of streamlines shows a big vortex in the middle of the cavity; therefore a part of the entering air is returned and goes out of the cavity. In the graph of isotherms a thermal stratification is observed in the half of the cavity near to the isothermal wall.

In Fig. 5, the temperature field and flow pattern results for Ra=10^7 and AR=4 are shown. It is observed in the stream-

lines and isotherms graphs for 45° and 90°, the presence of complex flow patterns due to the formation of multiple vortexes and thermal plumes. The thermal plumes travel driven by the incoming air and reach the isothermal wall, making the flow unstable. When the angle is 135°, the graph of streamlines shows the presence of two vortexes, one in the top corner and other in the center of the cavity, therefore only a small part of the ingoing cold air reaches the isothermal wall, most of it turns around and comes out in an oblique form.

In the Table III are presented the average Nusselt numbers (convective, radiative and total) as a function of: Rayleigh number, the inclination angle and the aspect ratio of the open cavity. It is noted that, in some cases the calculations of the convective Nusselt numbers not reached the steady state, this is explained by the periodic formation of thermal plumes in the bottom adiabatic wall that travels and mix with the thermal boundary layer of the isothermal wall. For these cases the mean values and the corresponding standard deviations are presented. It is observed that the values of the average convective Nusselt number and the total Nusselt number, varied significantly with respect to the inclination angle and the aspect ratio of the cavity. The average convective Nusselt number for angles of 45° and 90° are considerable higher that those corresponding to an inclination angle of 135°, therefore orientations of 45° and 90° favored the heat transfer by natural convection, while an orientations of 135° hindered it. For a fixed aspect ratio and Rayleigh number, the average radiative Nusselt number stayed constant for all the angles considered in the study. The values of the average radiative Nusselt number were always bigger than the average convective Nusselt number. This fact indicates that the exchange of thermal radiation between walls is quantitative more relevant that the convective phenomenon. The minimum values of the total Nusselt for each aspect ratio number occurred at ϕ=135°, for this inclination angle the radiative Nusselt number is greater than the convective Nusselt number between 1337 % (AR=2) and 1191% (AR=4). On the other hand, when the aspect increases its value, most of the average Nusselt numbers reduce its values (except the average convective Nusselt number for Ra=10^6).

Finally the comparison between the average convective Nusselt numbers obtained by Mohamad [13] in Table II and the average convective and total Nusselt numbers (corresponding to the same inclination angle and Rayleigh number) reported in Table 3, shows that when the radiative exchange was considered the average convective Nusselt number reduced between 17.1% (Ra=10^7) and 39% (Ra=10^5), however the total average Nusselt numbers increased among 41.4% (Ra=10^5) and 80.6% (Ra=10^7). Because an emissivity of the surfaces equal to 1 was considered to obtain the above results, the previous results represent the maximum expected differences.

5. Conclusions

In this paper the numerical calculations of the heat transfer by natural convection and surface thermal radiation in a tilted open shallow cavity were presented. Based on the obtained results, the conclusions of this work are the following:

The temperature field and the flow pattern are very sensitive to the orientation of the cavity.

It is appreciated for inclination angles of 45° (AR=4) and 90° (AR of 2 and 4) the formation of thermal plumes in the bottom adiabatic wall that travel and mix with the thermal layer of the hot wall, causing oscillations in the convective Nusselt number.

The values of the average convective Nusselt number and the total Nusselt number, varied significantly with respect to the inclination angle. The angles of 45° and 90° favored the heat transfer by natural convection, while the angle of 135° hindered it.

The values of the total average Nusselt numbers reduce when the aspect ratio increases its value.

In this heat transfer problem, the exchange of thermal radiation between walls is considerably more relevant that the convective phenomenon for and inclination angle of 135°.

Nomenclature

F_{ij}	view factor between surface i and surface j.
g	gravitational acceleration [m s^{-2}]
H	heigth of the cavity [m]
J	radiosity [W m^{-2}]
k	thermal conductivity [W m^{-1} K^{-1}]
L	length of the cavity [m]
Nr	conduction-radiation number (=$\sigma T_H^4 L/k\,(T_H - T_\infty)$) [-]
Nu	local Nusselt number [-]
$\overline{Nu}$	average Nusselt number [-]
P	pressure [N/m^2]
P	dimensionless pressure (=p-$p_\infty/\rho u_\infty^2$) [-]
Pr	Prandtl number (=ν/α) [-]
Q_r	dimensionless net radiative heat flux (=$q_r/\sigma T_H^4$) [-]
Ra	Rayleigh number [-]
T	absolute temperature [K]
T_H	temperature of the heated wall [K]
T_∞	temperature of the environment [K]
t	time [s]
U_o	reference convective velocity [m s^{-1}]
u	component-x of velocity [m s^{-1}]
v	component-y of velocity [m s^{-1}]
U	dimensionless velocity components [-]
V	dimensionless velocity components [-]
x	coordinate system [m]
y	coordinate system [m]
X	dimensionless coordinates [-]
Y	dimensionless coordinates [-]

Greek symbols

α thermal diffusivity [$m^2\ s^{-1}$]

β thermal expansion coefficient [K^{-1}]

ε emissivity of the surface [-]

ϕ inclination angle of the cavity [-]

ν kinematic viscosity [$m^2\ s^{-1}$]

θ dimensionless temperature [-]

σ Stefan-Boltzmann constant [$W\ m^{-2}\ K^{-1}$]

τ dimensionless time [-]

1. P. Le Quere, J.A Humphrey, and F.S. Sherman, *Numer. Heat Tr.* **4** (1981) 249.
2. F. Penot, *Numer. Heat Tr.* **5** (1982) 421.
3. Y.L. Chan and C.L. Tien, *Numer. Heat Tr.* **8** (1985) 65.
4. Y.L. Chan and C.L. Tien, *Int. J. Heat Mass Transfer* **28** (1985) 603.
5. J.A. Humphrey and W.M. To, *Int. J. Heat Mass Transfer* **29** (1986) 593.
6. M. Miyamoto, T.H. Kuehn, R.J. Goldstein, and Y. Katoh, *Numer. Heat Tr. A-Appl.* **15** (1989) 411.
7. K. Vafai and J. Ettefagh, *Int. J. Heat Mass Transfer*, 33 (1990) 2311.
8. K. Vafai and J. Ettefagh, *Int. J. Heat Mass Transfer* **33** (1990) 2329.
9. J.L. Lage, J.S. Lim, and A. Bejan, *J. Heat Trans-T ASME* **114** (1992) 479.
10. D. Angirasa, M.J. Pourquié, and F.T. Nieuwstadt, *Numerical Heat Transfer Part A* **22** (1992) 223.
11. C. Balaji and S.P. Venkateshan, *Int. J. Heat Fluid Flow* **15** (1994) 317.
12. C. Balaji and S.P. Venkateshan, *Int. J. Heat Fluid Flow* **16** (1995) 139.
13. A.A. Mohamad, *Numer. Heat Tr. A-Appl.* **27** (1995) 705.
14. D. Angirasa, J.G. Eggels, and F.T. Nieuwstadt, *Numer. Heat Tr. A-Appl.* **28** (1995) 755.
15. A.H. Abib and Y. Jaluria, *Int. J. Heat Mass Transfer* **38** (1995) 2489.
16. I. Sezai and A.A. Mohamad, *Int. J. Numerical Methods Heat Fluid Flow* **8** (1998) 800.
17. K. Khanafer and K. Vafai, *Int. J. Heat Mass Transfer* **43** (2000) 4087.
18. K. Khanafer and K. Vafai, *Int. J. Heat Mass Transfer*, **45** (2002) 2527.
19. K. Khanafer, K. Vafai, and M. Lighstone, *Int. J. Heat Mass Transfer* **45** (2002) 5171.
20. O. Polat and E. Bilgen, *Int. J. Therm. Sci.* **41** (2002) 360.
21. O. Polat and E. Bilgen, *Int. J. Heat Mass Transfer* **46** (2003) 1563.
22. S.N. Singh and S.P. Venkateshan, *Int. J. Therm. Sci.* **43** (2004) 865.
23. E. Bilgen and H. Oztop, *Int. J. Heat Mass Transfer* **48** (2005) 1470.
24. J.F. Hinojosa, R.E. Cabanillas, G. Alvarez, and C.A. Estrada, *Int. Commun. Heat Mass* **32** (2005) 1184.
25. J.F. Hinojosa, R.E. Cabanillas, G. Alvarez, and C.A. Estrada, *Numer. Heat Tr. A-Appl.* **48** (2005) 179.
26. J.F. Hinojosa, G. Alvarez, and C.A. Estrada, *Rev. Mex. Fis.* **52** (2006) 111.
27. H. Nouaneguea, A. Muftuoglua, and E. Bilgen, *Int. J. Heat Mass Transfer* **51** (2008) 6054.
28. A. Koca, *Int. Commun. Heat Mass* **35** (2008) 1385.
29. A.A. Mohamad, M. El-Ganaoui, and R. Bennacer, *Int. J. Therm. Sci.* **48** (2009) 1870.
30. S.K.S. Boetcher and E.M. Sparrow, *Int. J. Heat Mass Transfer* **52** (2009) 3850.
31. J.F. Hinojosa and J. Cervantes de Gortari, *Heat Mass Transfer* **46** (2010) 595.
32. M.A. Hossain, S. Asghar and R.S.R. Gorla, *Int. J. Numerical Methods Heat Fluid Flow* **20** (2010) 759.
33. A.A. Mohamad and A. Kuzmin, *Int. J. Heat Mass Transfer,* **53** (2010) 990.
34. A. Andreozzi and O. Manca, *Numer. Heat Tr. A-Appl.*, **57** (2010) 453.
35. J.O. Juárez, J.F. Hinojosa, J.P. Xamán, and M. Pérez, *Int. J. Therm. Sci.*, **50** (2011) 2184.
36. M. Modest, *Radiative Heat Transfer* (McGraw-Hill, New York, USA, 1993).
37. P.H. Gaskell and A.K.C. Lau, *Int. J. Numerical Methods Fluids* **8** (1988) 617.
38. J.P. Van Doormaal and G.D. Raithby, *Numer. Heat Tr.* **7** (1984) 147.
39. H.L. Stone, *J. Numer. Analysis* **5** (1968) 530.
40. A. Sanchez and T. Smith, *J. Heat Trans-T ASME* **114** (1992) 465-472.